This is a preprint, the final version is subject to change, of the American Mineralogist (MSA)
Cite as Authors (Year) Title. American Mineralogist, in press.
(DOI will not work until issue is live.) DOI: http://dx.doi.org/10.2138/am-2016-5635

Oxygen diffusion and exchange in dolomite rock at 700 °C, 100 MPa

Michael T. DeAngelis[1*]

Theodore C. Labotka[2]

Mostafa Fayek[3]

David R. Cole[4]

Lawrence M. Anovitz[5]

[1]Department of Earth Sciences, University of Arkansas at Little Rock, Little Rock, Arkansas 72204-1000, USA

[2]Department of Earth and Planetary Sciences, University of Tennessee, Knoxville, Tennessee 37996-1410, USA

[3]Department of Geological Sciences, University of Manitoba, Winnipeg, Manitoba R3T 2N2, Canada

[4]School of Earth Sciences, The Ohio State University, Columbus, Ohio, 43210-1398, USA

[5]Chemical Sciences Division, Oak Ridge National Laboratory, Oak Ridge, Tennessee 37831-6110, USA

[*]Corresponding Author
mtdeangelis@ualr.edu
Ph (501) 569-3542
Fax (501) 569-3271

This is a preprint, the final version is subject to change, of the American Mineralogist (MSA)
Cite as Authors (Year) Title. American Mineralogist, in press.
(DOI will not work until issue is live.) DOI: http://dx.doi.org/10.2138/am-2016-5635

Abstract

In contact-metamorphic environments, dolomite commonly breaks down to calcite + periclase + CO_2 as a result of the infiltration of H_2O. The transport and exchange of oxygen in dolomite rock during the breakdown reaction were examined experimentally by reacting a cylindrical core of Reed Dolomite with isotopically enriched water having the composition $HD^{18}O_{0.5}{}^{16}O_{0.5}$ at 700 °C and 100 MPa for 29 days. Reaction products formed along grain boundaries, fractures, and on the outside surface of the core. Some dolomite grains became enriched in Fe as a result of replacement of the host dolomite. Extensive voids are found in the grain boundaries as a result of the $\sim 25\%$ loss in solid volume during reaction. There are also pores, ~ 1 μm in diameter, in the dolomite, notably in the vicinity of the replaced dolomite. The distribution of ^{18}O in the dolomite and reaction products was used as a tracer of the transport and exchange of O during reaction. Electron probe microanalysis (EPMA) and secondary ion mass spectrometry (SIMS) analyses showed pervasive infiltration of fluid along grain boundaries and fractures, growth and isotopic exchange with products of reaction, and diffusion of ^{18}O into dolomite grains. The fluid infiltrated efficiently along grain boundaries to the dolomite grain surface. The host dolomite shows an enrichment in ^{18}O along grain boundaries, indicating a diffusive exchange with the fluid. An estimate of the diffusion coefficient of oxygen in dolomite, determined from ion probe spot analyses, gives $D \approx 1 \times 10^{-12}$ mm^2/s. This value is comparable to the oxygen diffusion coefficient for calcite in an H_2O-rich fluid. Mass balance of O in the experiment, including dolomite–fluid exchange, the amounts of neomorphic reaction products, and the fluid components, indicates that the reaction products have a ^{18}O concentration only about half that of the fluid. Ion probe spot analyses of calcite from both the center and the edge of the core have the fraction $F = {}^{18}O/({}^{18}O+{}^{16}O)$ of 0.14 ± 0.1; whereas, the value calculated for the fluid is 0.31. The measured F values of calcite are intermediate between the initial F values of starting water and

This is a preprint, the final version is subject to change, of the American Mineralogist (MSA)
Cite as Authors (Year) Title. American Mineralogist, in press.
(DOI will not work until issue is live.) DOI: http://dx.doi.org/10.2138/am-2016-5635

dolomite, indicating that the reaction products record a mix of both dolomite- and fluid-derived oxygen. The products reached about 45% of isotopic equilibrium, similar to the extent of the mineral–fluid reaction. The Fe-rich, replacement dolomite near the core edge has an elevated value of $F = 0.02 \pm 0.002$, ten times the value of $F \approx 0.002$ for unreacted dolomite, but less than the value for the calcite. The distribution of ^{18}O in the minerals indicates that the breakdown and replacement reactions were faster than O diffusion in dolomite.

KEYWORDS: dolomite, oxygen isotope, exchange, diffusion, contact metamorphism, SIMS

This is a preprint, the final version is subject to change, of the American Mineralogist (MSA)
Cite as Authors (Year) Title. American Mineralogist, in press.
(DOI will not work until issue is live.) DOI: http://dx.doi.org/10.2138/am-2016-5635

Introduction

Oxygen isotopes are useful tracers of fluid transport and exchange in contact metamorphic aureoles because there can be significant isotopic contrast between magmatic fluids associated with an intruding pluton and the minerals and fluids in the host rock (Baumgartner and Ferry 1991, Baumgartner and Rumble 1988, Bowman et al., 1994, Cook and Bowman 1994, Ferry 1991, Moore and Kerrick 1976, Nabelek et al. 1984, Nabelek 1991, Roselle et al. 1999, Valley et al. 1986, Valley 2001). The rates of isotope exchange can be relatively fast in some contact metamorphic environments (e.g. Bowman et al. 2009), but vary depending on the mechanisms for exchange. Exchange mechanisms in contact metamorphic aureoles can include: neomorphic exchange (i.e. isotope exchange during the reactive growth of new minerals), recrystallization, and diffusive exchange (e.g. Eiler et al. 1995, Gerdes et al. 1999). It is likely that no single mechanism is totally responsible for the redistribution of oxygen isotopes in rock-water systems far from equilibrium. Therefore, all possible mechanistic pathways should be considered to fully describe exchange.

The intent of this study is to examine experimentally these mechanisms for exchange of oxygen between fluids and carbonate host rocks during contact metamorphism. Several contact metamorphic analog experiments using dolomite rock cores were previously performed to determine kinetic variables such as reaction rates, extent of reaction, activation energies and mechanisms of mineral reaction (see DeAngelis et al. 2007). We selected experiment MR6 from that study to examine in more detail because it contains both reaction-rich and reaction-free zones; some dolomite grains adjacent to reaction zones show replacement textures, while other dolomite grains around these zones are unchanged. The presence of these different zones within one sample has allowed us to examine the three exchange mechanisms described above. We find that oxygen in neomorphic crystals is both dolomite- and fluid-derived, that recrystallization resulted in ^{18}O-enriched dolomite, and that diffusive exchange oc-

curred in dolomite adjacent to both reactive and non-reactive grain boundaries.

Methods

Experimental techniques

The experiment was conducted using the Late Proterozoic Reed Dolomite from Nevada as starting material. The Reed Dolomite is a massive, brown to tan, medium- to coarse-grained dolomitic marble (Richards et al. 1996). The grain size ranges from 0.5 to 1.0 mm in diameter, and the grains are anhedral in shape. This sample also contains minor quartz veins, trace pyrite, and intergranular fractures. Average ^{18}O values of the Reed Dolomite ranges from 11.1 to 21.5‰ (SMOW) (Richards et al. 1996).

A small core, approximately 4 mm in diameter and 6 mm in length, was drilled from the marble sample. The core was placed in a thin-walled, 5 mm gold capsule, approximately 7.5 cm in length. An aliquot (0.03805 g) of $HD^{18}O_{0.5}{}^{16}O_{0.5}$ was added to the sample, and the capsule was purged with CO_2 gas and arc-welded closed. The prepared capsule was placed in a vacuum oven for approximately 24 hours and then reweighed to ensure that there were no leaks. The capsule was then placed in a cold-seal hydrothermal apparatus, heated and pressurized to 700 °C and 100 MPa, and held at this condition for 29 days. The experiment was heated to the desired temperature over a period of thirty to forty minutes. During the course of the experiment, both pressure and temperature were monitored and recorded. The experiment was isobarically quenched to ambient temperature over a period of twenty minutes. The capsule was then removed from the hydrothermal apparatus, weighed to test for leakage, and punctured under vacuum. Any water present was cryogenically captured, and any reaction produced CO_2 was measured by manometry. The dolomite

This is a preprint, the final version is subject to change, of the American Mineralogist (MSA)
Cite as Authors (Year) Title. American Mineralogist, in press.
(DOI will not work until issue is live.) DOI: http://dx.doi.org/10.2138/am-2016-5635

core was then removed from the gold capsule, embedded in epoxy, and sectioned longitudinally.

Analytical techniques

Reaction products, reaction textures, and extent of reaction were determined by petrography and EPMA. Back-scattered electron (BSE) and Ca, Mg, Si, and Fe Kα X-ray images were collected with the Cameca SX-100 at the University of Tennessee. For these analyses, the microprobe had an accelerating voltage potential of 15 kV, a beam current of 4 nA, and a beam size of 1 µm. Images were generated by rastering the sample stage over a 512×512 µm area using a 2 µm step and a counting time of 1 ms per step. Quantitative mineral analyses were also collected, and for these analyses the microprobe had an accelerating voltage potential of 15 kV, a beam current of 6 nA, a beam size of 1 µm, and a counting time of 40 s for most elements. Natural standards of calcite, dolomite, and periclase were used for calibration.

Oxygen isotope distributions were obtained by ion imaging and isotope ratio analysis using the CAMECA ims 7f SIMS located in the Manitoba Regional Materials and Surface Characterization Facility at the University of Manitoba, Canada. The sample was prepared by applying a thin gold coat ($\sim$ 15 s of sputtering time) to a thin section mount. Oxygen isotope (^{18}O and ^{16}O) ion images were generated by rastering over a 250×250 µm area using a 150 pA Cs^+ primary beam and a 200 V high voltage energy offset. Oxygen-isotope ratio spot analyses of the sample, dolomite standards (MD Dolomite: $\delta^{18}O_{SMOW} = 21.9‰$; Brumado Dolomite: $\delta^{18}O_{SMOW} = 14.0‰$), and a calcite standard (Joplin Calcite: $\delta^{18}O_{SMOW} = 5.8‰$) were measured using a 300 pA Cs^+ primary beam and 200 volt energy offset. This primary beam current was selected to keep the spot size small (10 µm); however, a minimum pre-sputtering period of 30 s was required to obtain a stable count rate ($\sim 1.5 \times 10^5$ counts on ^{16}O)

This is a preprint, the final version is subject to change, of the American Mineralogist (MSA)
Cite as Authors (Year) Title. American Mineralogist, in press.
(DOI will not work until issue is live.) DOI: http://dx.doi.org/10.2138/am-2016-5635

before collecting oxygen isotope ratio spot analyses.

To compare mineral composition in reaction zones with areas of isotope transport and exchange, X-ray and ion images were co-registered with use of the program ENVI by selecting corresponding control points and resizing the ion image to match X-ray image dimensions.

Results

Reaction products and textures

Areas of reaction are present throughout sample MR6 (Fig. 1). The total fraction of dolomite that reacted was previously determined by EPMA point counting to be 0.19 (Table 3 in DeAngelis et al. 2007). Because the fluid–solid molar ratio in this experiment was only 1.5, that extent of reaction corresponds to a fraction of the equilibrium value of 0.46. The most extensive reaction occurred in the fluid-accessible areas near the edges of the core; however, limited reaction is also present toward the interior of the core where fluid was localized along grain boundaries and fractures. A thin quartz vein is present through the center of the core, and some additional reaction occurred in and around this vein. Primary products of reaction are calcite and periclase, with minor amounts of other hydrated Mg-carbonates (e.g. nesquehonite [$MgCO_3 \cdot 3H_2O$] as an exterior quench phase) and some Mg-silicates (e.g. forsterite adjacent to the quartz vein). The two areas selected for detailed analysis of ^{18}O and ^{16}O distributions are shown in Figure 1.

The area shown in Figure 2 is in the interior of the core where unreacted dolomite grains are partly replaced by calcite and periclase along some grain boundaries. Other grain boundaries appear to be reaction-free. The X-ray image in Figure 2A shows the typical mottled appearance of a grain boundary reaction zone, with small (10–20

This is a preprint, the final version is subject to change, of the American Mineralogist (MSA)
Cite as Authors (Year) Title. American Mineralogist, in press.
(DOI will not work until issue is live.) DOI: http://dx.doi.org/10.2138/am-2016-5635

µm), anhedral calcite and periclase grains interspersed with void space between the dolomite grains. Pores also mark the boundary between the host dolomite and the reaction rim, although they are small in Figure 2A. Dolomite rims are not altered everywhere, as can be seen at the right edge of Figure 2.

The area displayed in Figure 3 is adjacent to a quartz vein, which contained a small amount of pyrite. The reaction products here contain calcite and periclase along the host dolomite grain boundaries, similar to the region shown in Figure 2. There are also some grains of forsterite and hydrated Mg carbonates in the reacted vein. Dolomite grains near the vein, though, also have regions enriched in Fe. These are seen as the slightly brighter areas in the BSE images. Quantitative analyses of the dolomite indicate that the amount of FeO is 1.0–1.4 wt%. The pyrite is thought to be the source of Fe found within the dolomite grains. The boundary between the Fe-enriched dolomite and the host dolomite is sharp. There is no particular concentration of pores at the boundary, although there are numerous pores, on the order of 1 μm in diameter, throughout the Fe dolomite and the host dolomite. It is difficult to see in Figure 3, but some of the pores in the host dolomite appear to have a small rim of the Fe dolomite.

^{18}O distribution

The average ^{18}O values of the Reed Dolomite range from 11.1‰ to 21.5‰ (Richards et al. 1996), therefore, the amount of ^{18}O in the starting water (50%) far exceeds the amount of ^{18}O in the original dolomite marble. Any significant increase in the ^{18}O at any location within the experiment cores, therefore, resulted from exchange with the fluid. Because the measured concentrations of ^{18}O span a large range, isotope ratio values reported here use the F notation [$F = {}^{18}\text{O}$ counts/(^{18}O+^{16}O) counts] instead of the more traditional δ^{18}O notation. For example, the F value range of unreacted

This is a preprint, the final version is subject to change, of the American Mineralogist (MSA)
Cite as Authors (Year) Title. American Mineralogist, in press.
(DOI will not work until issue is live.) DOI: http://dx.doi.org/10.2138/am-2016-5635

Reed Dolomite based on the δ^{18}O values above is $F = 0.00194 \pm 0.0005$. An additional consequence of using this isotopically enriched starting water and reporting values with the F notation is that the equilibrium fractionation between any of the minerals and the fluid phase is negligible when compared with the difference in F between the starting dolomite and fluid in the experiment.

O-isotope imagery. Qualitative O-isotope ion images can be useful to observe ^{18}O distribution (e.g. Labotka et al. 2007), and have been generated in select zones within Figures 2 and 3 (Figs. 2B and 3B). The dimensions of the ion images are smaller than the dimensions for X-ray and BSE images, so only a portion of the BSE images in Figures 2B and 3B are overlain by ion images.

The O-isotope ion-image overlay in Figure 2B shows the distribution of ^{18}O along a portion of a grain-boundary reaction zone near the center of sample MR6. The background BSE image in Figure 2B shows an area of transition from abundant reaction products along grain boundaries in the upper left and middle that thins to a reaction-free area along the grain boundary to the lower right. The purple-colored areas of the overlain ion image coincide with the location of reaction products in the BSE image, showing that reaction products are characterized by a significant increase in ^{18}O acquired during growth. Areas of ^{18}O enrichment also appear along the grain boundary in the reaction-free zone to the lower right, indicating grain boundary diffusion of an ^{18}O-rich fluid despite the lack of reaction products. The orange-colored areas of the overlain ion image also indicate elevated values of ^{18}O extending into the dolomite grains adjacent to the grain boundary zone. Because there is no evidence for recrystallization of the dolomite immediately adjacent to the reaction rim, the increase in ^{18}O is likely the result of diffusive exchange between the fluid and the unreacted dolomite. Similar to Figure 2B, the ion image overlay in Figure 3B also indicates significant ^{18}O enrichment in the reaction products, but also shows greater

This is a preprint, the final version is subject to change, of the American Mineralogist (MSA)
Cite as Authors (Year) Title. American Mineralogist, in press.
(DOI will not work until issue is live.) DOI: http://dx.doi.org/10.2138/am-2016-5635

enrichment extending into dolomite grains near the outer edge of the core.

O-isotope spot analyses. Because ^{18}O is much more concentrated in the reaction products than in the host dolomite grains, there is a lower threshold of ^{18}O concentration ($F \approx 0.10$) that can be observed in these ion images. To obtain more detailed resolution, spot analyses were performed to quantify ^{18}O concentrations.

Detailed O-isotope spot analyses were performed on reaction products, unreacted dolomite, and replaced dolomite (Table 1). The calcite (cc1–2) in the grain boundary reaction zone in the interior of the core (Figure 2) has an average value of $F = 0.14$ ($n = 2$). Calcite grains within the grain boundary reaction zone (cc3–5) near the vein (Figure 3B) have a similar average value of $F = 0.15$ ($n = 3$). Because these calcite grains are small (10–20 µm), it is possible that these analyses represent mixtures of oxygen values from several grains. However, since the equilibrium fractionation is negligible compared with determined F values, the average value for all spots measured on calcite, $F = 0.14 \pm 0.1$ ($n = 5$), justifiably represents the value of all nearby reaction products. The periclase and nesquehonite in both reaction areas were indeed too small to analyze by SIMS spot analysis. However, since they were also exchanging with the fluid during formation, they are also expected to have O-isotope values that are similarly enriched.

O-isotope spot-analyses were collected along three traverses (A, B, C) in the dolomite grain immediately adjacent to the grain boundary reaction zone in Figure 2. Each traverse started approximately 15 µm inside the grain boundary edge of the dolomite and each spot was collected in 20 µm steps advancing toward the dolomite grain center. These traverses exhibit increased F values in the dolomite near the grain boundary that decrease toward the grain core. There are also lateral differences between these traverses, with Traverse B, which originates adjacent to the most highly reacted zone, showing slightly increased F values over Traverse C, the

214 traverse adjacent to the reaction-free zone.

215 O-isotope spot-analyses were also collected along four traverses (D, E, F, G)
216 through the dolomite grain shown in Figure 3 near the edge of the dolomite core.
217 Traverse D contains three spots beginning at a grain boundary and traversing to-
218 ward the center of the unreacted portion of the dolomite grain. The rim value of this
219 traverse is elevated adjacent to the grain boundary ($F = 0.049$), but drops to the
220 unreacted value for the dolomite grains ($F \approx 0.002$). Traverse E contains three spots
221 analyzed in the replaced portion of the dolomite. These analyses show an average en-
222 richment of $F = 0.02 \pm 0.002$ (n=3), about ten times the host dolomite value. Spots
223 along two additional traverses (F, G) were analyzed from the reaction zone on the
224 right side of dolomite grain through the replaced and host portions of the dolomite
225 grain and ending near the grain boundary on the left side of the grain. These tra-
226 verses have elevated values for the spots analyzed in the replacement region, similar
227 to traverse E, background values for the unreacted areas (similar to points D2 and
228 D3), and greatly enriched values for the analyses immediately adjacent to reaction
229 products near the edges of the dolomite grain (similar to point D1).

This is a preprint, the final version is subject to change, of the American Mineralogist (MSA)
Cite as Authors (Year) Title. American Mineralogist, in press.
(DOI will not work until issue is live.) DOI: http://dx.doi.org/10.2138/am-2016-5635

Discussion

The textures and the distribution of regions of enrichment in ^{18}O shown in Figures 2 and 3 indicate that H_2O permeated the grain boundaries deep within the sample. The reaction products calcite and periclase crystallized along the boundaries, those reaction products became enriched in ^{18}O, and the host dolomite exchanged oxygen with the fluid. Dolomite in portions of the sample near the pyrite-bearing vein appears to have recrystallized, acquiring an elevated Fe content and becoming enriched in ^{18}O.

We wish to account for the redistribution of O that occurred during these processes, to estimate the magnitude of the diffusivity of O in dolomite, and determine the O exchange during recrystallization of dolomite near the vein.

Diffusion in dolomite

The SIMS ion image and spot analyses of an interior dolomite grain, Traverses A–C (Fig. 2B), show that ^{18}O enriched near the edge of the dolomite, even where there is no evidence for the breakdown reaction (Fig. 2A). The fraction of ^{18}O decreases toward the interior of the grain, as in a diffusive exchange with O in the grain-boundary fluid. Although the data do not permit a precise determination of the diffusion coefficient D, they provide some limits on the possible value of D. With the recognition that one spot at the edge of the dolomite grain might contain O from the reaction zone, the analyses can be compared with values predicted by simple diffusion models. The experiment is a closed system, and the dolomite grains are roughly spherical. The fluid had an initial $^{18}O/^{16}O$ ratio of 0.5, but that changed as reaction proceeded. During reaction, the dolomite–matrix interface retreated, but that shrinking was slow enough that a diffusion profile was preserved. A good model for this experiment is diffusion from a well stirred reservoir of limited size into a sphere. The solution to this problem

This is a preprint, the final version is subject to change, of the American Mineralogist (MSA)
Cite as Authors (Year) Title. American Mineralogist, in press.
(DOI will not work until issue is live.) DOI: http://dx.doi.org/10.2138/am-2016-5635

is given by Crank (1975). The fraction of ^{18}O at any time t is

$$F_{\mathrm{t}}(r) = F_{\infty}\left[1 + \sum_{n=1}^{\infty} \frac{6(1+\alpha)\exp(-Dq_n^2 t/a^2)}{9 + 9\alpha + q_n^2\alpha^2} \frac{a}{r} \frac{\sin(q_n r/a)}{\sin q_n}\right] + F_0 \qquad (1)$$

where $F_{\mathrm{t}}(r)$ is the value at the end of the experiment and at a radius r. F_{∞} is the value for the whole system at infinite time (0.099). F_0 is the initial value for dolomite (0.002). D is the oxygen diffusion coefficient, and a is the radius of the grain (0.5 mm); α is the ratio of the moles of O in the fluid and solid at the end of the experiment (0.33), and t is the duration of the experiment. The values for q_n are determined from the positive, non-zero roots of (Crank 1975)

$$\tan q_n = \frac{3q_n}{3 + \alpha q_n^2} \qquad (2)$$

Figure 4 shows the data from Figure 2 in comparison with the solutions from Equation 1 for various values of D. The data fall between 10^{-12} and 10^{-10} mm^2/s, with most corresponding to a value of D of 10^{-11} mm^2/s.

Equation 1 is used to calculate diffusion profiles for values of D that bracket the data. The diffusion depth, however, is shallow, $\lesssim 20$ µm, relative to the radius of the grain, 500 µm. A value of D, then, can also be estimated from an inversion of the data with a simple infinite half-space solution, $C = C_0\ \mathrm{erfc}[x/(2\sqrt{Dt})]$, where C_0 is the fixed concentration at the surface. Fitting the data from Figure 2 with a nonlinear least-squares method gives a diffusivity of $D = 1.8 \times 10^{-12}$ mm^2/s, with an error of ±9%. While not precisely determined by our data, the estimated value is similar to the diffusivity of O in calcite under the same conditions (Labotka et al. 2011).

This is a preprint, the final version is subject to change, of the American Mineralogist (MSA)
Cite as Authors (Year) Title. American Mineralogist, in press.
(DOI will not work until issue is live.) DOI: http://dx.doi.org/10.2138/am-2016-5635

Oxygen isotope mass balance

In this experiment, dolomite was placed in a volume of water, with which it was out of equilibrium at 100 MPa and 700 °C, in terms of both fluid composition (x_{CO_2}) and isotopic composition ($^{18}O/^{16}O$). The fractional extent of mineral reaction, 0.19, was almost half of the equilibrium value (0.41), resulting in the mixture of dolomite, calcite, and periclase (DeAngelis et al. 2007). The distribution of ^{18}O among the product phases should determine the degree of approach to isotopic equilibrium.

The mass balance of O before and after reaction is given in Table 2. The starting distribution of ^{18}O is simply the amount in the water, with the simple assumption that relative to the amount in the fluid, the amount in the dolomite is zero. With 38.05 mg of $HD^{18}O_{0.5}{}^{16}O_{0.5}$ and 122.73 mg of dolomite, The total amounts of ^{18}O and ^{16}O are 17.12 mg and 137.95 mg, respectively.

After reaction, ^{18}O is redistributed among the product minerals, the Fe-enriched dolomite, and the fluid. The amounts of the Fe dolomite and quench products are small and are excluded from the mass balance. The composition of the fluid after the experiment was not measured, so the fluid composition shown in Table 2 was determined by difference. The amounts of calcite and periclase and the amount of CO_2 added to the fluid during reaction were determined by the measured fractional extent of reaction, 0.19 (DeAngelis et al. 2007). The isotopic composition of calcite was measured ($F = 0.14$). The composition of periclase was not measured but was assumed to be the same as that of calcite.

The uptake of ^{18}O by the dolomite from the fluid and the loss of ^{16}O to the fluid from the dolomite were calculated with Equation 6.30 in Crank (1975), which is an integrated form of Equation 1, and with an approximate average oxygen diffusion coefficient of $D = 5.0\times10^{-12}$ mm^2/s. The result is a total uptake value of $F_{\text{total}} = 0.009$ by the host dolomite.

The resulting mass balance for O is shown in Table 2, in which the values are

This is a preprint, the final version is subject to change, of the American Mineralogist (MSA)
Cite as Authors (Year) Title. American Mineralogist, in press.
(DOI will not work until issue is live.) DOI: http://dx.doi.org/10.2138/am-2016-5635

given in mass units. The mass of ^{18}O and ^{16}O in the fluid calculated by difference indicates a composition of $F = 0.31$. This is more than twice the value measured in the product calcite. The reaction products have reached only about 45% of the equilibrium isotopic value, which, coincidentally, is the percentage of the approach of the sample to mineralogical equilibrium.

Oxygen isotope distribution in replacement dolomite

The Fe-bearing dolomite near the vein shows the textural characteristics of replacement of the host dolomite by the Fe-rich variety. The boundary between them is sharp. A compositional profile along the line A–A′, Figure 5, shows that FeO is present at the 1.0 wt% level in the Fe dolomite but is only about 0.1 wt% in the host dolomite. There seems to be a decrease in FeO in the Fe dolomite from $\sim$ 1.2% at the rim to $\sim$ 0.9% at the boundary of the host dolomite, although the trend is noisy. The drop to the host dolomite value is discontinuous at the resolution of the analytical points, 2 µm. This kind of replacement is seen in many natural and experimental mineral–fluid systems (Cole et al. 2004, Labotka et al. 2004, Putnis 2009, Jonas et al. 2015).

There is insufficient contrast in the ion image, Figure 3B, to pick out the boundary between the host and replacement dolomite, but the difference in ^{18}O abundance can be seen in the spot analyses. These are plotted in Figure 5B, as projected along the line A–A′. The points are broad, and there is some scatter in the values, but the replacement dolomite certainly seems to be elevated in its F value relative to the host dolomite. For example, the points along Traverse E have significantly higher F values ($F = 0.02 \pm 0.002$) than the adjacent host dolomite ($F \approx 0.002$). The break in ^{18}O composition also appears to be abrupt at the boundary between host and replacement. The available data do not indicate any diffusion of O into the host

This is a preprint, the final version is subject to change, of the American Mineralogist (MSA)
Cite as Authors (Year) Title. American Mineralogist, in press.
(DOI will not work until issue is live.) DOI: http://dx.doi.org/10.2138/am-2016-5635

dolomite across the replacement front, unlike the dolomite next to a grain boundary or fracture.

Implications

There are two kinds of heterogeneous reactions that affected the host dolomite. Throughout the core, dolomite broke down to calcite and periclase as a result of the presence of the H_2O fluid. Near the pyrite-bearing quartz vein, the host dolomite was partly replaced by dolomite with an elevated Fe content. O appears to have behaved differently in the two reactions. The dolomite breakdown reaction generated a large amount of porosity because the ΔV_{solid} is -24%. That and the porosity along the grain boundaries even where there was little or no reaction apparently permitted the host dolomite to exchange with the pore fluid, resulting in a small but noticeable diffusion profile in the dolomite. The diffusion depth in the dolomite is similar to that in calcite under the same conditions (Labotka et al. 2011), although the dolomite data are sparse. The fluid had ready access to the dolomite surface, even within the core.

The replacement reaction front shows no evidence for diffusion of O into the host dolomite. The ΔV_{solid} of the replacement reaction is small, estimated to be 4% of difference between dolomite and ankerite, $+0.1\%$. Fluid access to the interface seems to have been much more restricted than at grain boundaries. The thickness of the replacement zone is about 60 µm (Fig. 5A), whereas the diffusion depth at dolomite grain boundary is less than 20 µm (Fig. 4), which suggests that the rate of advancement of the reaction front was 2–3 times greater than the rate of diffusion. A diffusion profile would not have been able to form.

The ^{18}O content of the reaction products, both in the dolomite breakdown reaction and in the replacement reaction, is elevated but not as enriched as the fluid compo-

sition. The calcite and, presumably, periclase have an $F \approx 0.14$, which is greater than that of the replacement Fe dolomite, ~ 0.02. Both are much less than the fluid composition of about 0.31. For the dolomite breakdown reaction, approximately half of the O derives from the dolomite and half from the fluid. Apparently the O from the dissolved dolomite did not mix thoroughly with the fluid before the calcite and periclase precipitated. Even less mixing seems to be recorded by the replacement Fe dolomite. There, dolomite is replacing dolomite with what Putnis and Putnis (2007) called interface-coupled dissolution–reprecipitation, in which dissolution of the host dolomite is immediately followed by precipitation of the Fe dolomite.

This experiment was performed at conditions far from equilibrium to promote reaction and isotopic exchange over the relatively short duration of the experiment. While the duration of the experiment may be short in comparison with the amount of time available for reaction and exchange in a contact-metamorphic aureole, the distribution of ^{18}O indicates the relative rates of the reactions. Diffusion of O in dolomite occurred at the leisurely pace of about 10^{-12} mm^2/s. The breakdown of dolomite was limited by diffusion of H_2O and CO_2 through the product rim, which occurred at the more rapid pace of about 10^{-10} mm^2/s (DeAngelis et al 2007). There is no quantitative estimate of the rate of Fe dolomite replacement reaction, but it must have been sufficiently rapid to prevent diffusion in the host dolomite and to limit the enrichment of ^{18}O in the replacement dolomite.

This is a preprint, the final version is subject to change, of the American Mineralogist (MSA)
Cite as Authors (Year) Title. American Mineralogist, in press.
(DOI will not work until issue is live.) DOI: http://dx.doi.org/10.2138/am-2016-5635

Acknowledgments

This study is a portion of M.T. DeAngelis's dissertation work at the University of Tennessee, Knoxville. Many thanks to Allan Patchen at the University of Tennessee for help with EPMA analyses, and to Sharon Hull, Brandi Shabaga and Rong Liu at the University of Manitoba for help with SIMS analyses. We sincerely appreciate the comments from the reviewers of previous versions of the manuscript: John Bowman, Thomas Müller, and Virginia Peterson. Funding for this work was provided by the National Science Foundation grant EAR-0087553 and the Division of Chemical Sciences, Geosciences, and Biosciences, Office of Basic Energy Sciences, U.S. Department of Energy. Oak Ridge National Laboratory is managed and operated by UT-Battelle for the U.S. Department of Energy under contract DE-AC05-00OR22725. D.R.C. was also supported by research sponsored by the Geosciences Program in the Division of Chemical Sciences, Geosciences, and Biosciences, Office of Basic Energy Sciences, U.S. Department of Energy through grant DE-SC0006878 and by the A. P. Sloan-funded Deep Carbon Observatory under grant 2013-6-1. Partial funding for this work was also provided by a NSERC Discovery Grant to Fayek. Certain commercial equipment, instruments, materials and software are identified in this paper to foster understanding. Such identification does not imply recommendation or endorsement by the Department of Energy or Oak Ridge National Laboratory, nor does it imply that that materials or equipment identified are necessarily the best available for the purpose.

This is a preprint, the final version is subject to change, of the American Mineralogist (MSA)
Cite as Authors (Year) Title. American Mineralogist, in press.
(DOI will not work until issue is live.) DOI: http://dx.doi.org/10.2138/am-2016-5635

References cited

Anderson, T.F. (1972) Self-diffusion of Carbon and Oxygen in Dolomite. Journal of Geophysical Research 77, 857–861.

Baumgartner, L.P. and Ferry, J.M (1991) A model for coupled fluid-flow and mixed-volatile mineral reactions with applications to regional metamorphism. Contributions to Mineralogy and Petrology 106, 273–285.

Baumgartner, L.P. and Rumble III, D. (1988) Transport of stable isotopes: I: Development of a kinetic continuum theory for stable isotope transport. Contributions to Mineralogy and Petrology 98, 417–430.

Bowman, J.R., Willett, S.D., Cook, S.J. (1994) Oxygen isotopic transport and exchange during fluid flow: One-dimensional models and applications. American Journal of Science 294, 1–55.

Bowman, J.R., Valley, J.W., Kita, N.T. (2009) Mechanisms of oxygen isotopic exchange and isotopic evolution of $^{18}O/^{16}O$-depleted periclase zone marbles in the Alta aureole, Utah: insights from ion microprobe analysis of calcite. Contributions to Mineralogy and Petrology 157, 77–93.

Cole, D.R., Larson, P.B., Riciputi, L.R., and Mora, C.I. (2004) Oxygen isotope zoning profiles in hydrothermally altered feldspars: Estimating the duration of water-rock interaction. Geology 32, 29–32.

Cook, S.J. and Bowman, J.R. (1994) Contact metamorphism surrounding the Alta stock: thermal constraints and evidence of advective heat transport from calcite-dolomite geothermometry. American Mineralogist 79, 513–525.

Crank, J. (1975) The mathematics of diffusion, 414 p. Clarendon Press, Oxford.

399 DeAngelis, M.T., Labotka, T.C., Cole, D.R., Fayek, M., Anovitz, L.M. (2007) Ex-
400 perimental investigation of the breakdown of dolomite in rock cores at 100 MPa,
401 650–750 °C. American Mineralogist 92, 510–517.

402 Eiler, J.M, Valley, J.W., Graham, C.M, Baumgartner, L.P. (1995) The oxygen isotope
403 anatomy of a slowly cooled metamorphic rock. American Mineralogist 80, 757–764.

404 Ferry, J.M. (1991) Dehydration and decarbonation reactions as a record of fluid in-
405 filtration. Reviews in Mineralogy 26, 351–391.

406 Gerdes, M.L., Baumgartner, L.P., Valley, J.W. (1999) Stable isotope evidence for
407 limited fluid flow through dolomitic marble in the Adamello contact aureole, Cima
408 Uzza, Italy. Journal of Petrology 40, 853–872.

409 Jonas, L., John, T., and Putnis, A. (2015) Influence of temperature and Cl on the
410 hydrothermal replacement of calcite by apatite and the development of porous
411 microstructures. American Mineralogist 98, 1516–1525.

412 Labotka, T.C., Cole, D.R., Fayek, M., Riciputi, L.R., and Stadermann, F.J. (2004)
413 Coupled cation and oxygen-isotope exchange between alkali feldspar and aqueous
414 chloride solution. American Mineralogist 89, 1822–1825.

415 Labotka, T.C., Cole, D.R., Fayek, M.J., Chacko, T. (2011) An experimental study of
416 the diffusion of C and O in calcite in mixed CO_2–H_2O fluid. American Mineralogist
417 96, 1262–1269.

418 Labotka, T.C., DeAngelis, M.T., Cole, D.R., Fayek, M., Riciputi, L.R., Ushikubo,
419 T., Kita, N.T., Valley, J.W. (2007) O isotope exchange during the breakdown of
420 dolomite: An experimental study. Geochimica et Cosmochimica Acta 71, Supple-
421 ment 1, Goldschmidt Conference Abstracts 2007, A534.

Moore, J.N., and Kerrick, D.M. (1976) Equilibria in siliceous dolomites of the Alta aureole, Utah. American Journal of Science 276, 502–524.

Nabelek, P.I. (1991) Stable Isotope Monitors. Reviews in Mineralogy 26, 395–435.

Nabelek, P.I., Labotka, T.C., O'Neil, J.R., and Papike, J.J. (1984) Contrasting fluid/rock interaction between the Notch Peak granitic intrusion and argillites and limestones in western Utah: Evidence from stable isotopes and phase assemblages. Contributions to Mineralogy and Petrology 86, 25–34.

Putnis, A. (2009) Mineral Replacement Reactions. Reviews in Mineralogy and Geochemistry 70, 87–124.

Putnis, A., and Putnis, C. (2007) The mechanism of reequilibration of solids in the presence of a fluid phase. Journal of Solid State Chemistry 180, 1783–1786.

Richards, I.J., Labotka, T.C., and Gregory, R.T. (1996) Contrasting stable isotope behavior between calcite and dolomite marbles, Lone Mountain, Nevada. Contributions to Mineralogy and Petrology 123, 202–221.

Roselle, G.T., Baumgartner, L.P., Valley, J.W. (1999) Stable isotope evidence of heterogeneous fluid infiltration at the Ubehebe Peak contact aureole, Death Valley National Park, California. American Journal of Science 299, 93–138.

Valley, J.W. (1986) Stable isotope geochemistry of metamorphic rocks. Reviews in Mineralogy 16, 445–490.

Valley, J.W. (2001) Stable isotope thermometry at high temperatures. Reviews in Mineralogy and Geochemistry 43, 365-414.

This is a preprint, the final version is subject to change, of the American Mineralogist (MSA)
Cite as Authors (Year) Title. American Mineralogist, in press.
(DOI will not work until issue is live.) DOI: http://dx.doi.org/10.2138/am-2016-5635

Figure Captions

Figure 1. Photomicrograph of sample MR6. Boxed areas show X-ray and SIMS analysis locations in Figure 2 and Figure 3.

Figure 2. Dolomite grain boundary near the center of the dolomite core that has unreacted dolomite with adjacent reacted and reaction-free zones. (A) Composite X-ray image showing the distribution of Ca (aqua), Mg (red), and Fe (light gray). (B) ^{18}O ion image overlay on a back-scattered electron (BSE) image showing the qualitative distribution of ^{18}O. The location of ion probe analyses on two calcite grains (cc1, cc2) and dolomite traverses A, B, and C are also labeled. F values of oxygen isotope ratio spots analyzed along traverses A, B, and C are given in Table 1. The dark areas are pores. They are abundant in the grain boundary and between the host dolomite and the reaction products. There are also µm-sized pores in the host dolomite, which may be visible in Figure 2B.

Figure 3. The edge of the dolomite core has unreacted host dolomite, Fe-bearing replacement dolomite, and abundant reaction products. (A) Composite X-ray image showing the distribution of Ca (aqua), Mg (red), and Fe (light gray); the A–A′ is the location of the EPMA traverse. (B) ^{18}O ion image overlay on a BSE image showing the qualitative distribution of ^{18}O. The locations of ion probe analyses on three calcite grains (cc3, cc4, cc5) and dolomite traverses D, E, F, and G are also labeled. The values of F along traverses D, E, F, and G are given in Table 1.

Figure 4. Four calculated oxygen diffusion profiles in unreacted dolomite for the range $D = 10^{-9}$–10^{-12} mm^2/s determined using the equation

This is a preprint, the final version is subject to change, of the American Mineralogist (MSA)
Cite as Authors (Year) Title. American Mineralogist, in press.
(DOI will not work until issue is live.) DOI: http://dx.doi.org/10.2138/am-2016-5635

for spherical diffusion from a well-stirred solution of limited volume (modified from Crank, 1975). Measured oxygen isotope spot analyses from Traverses A, B, and C in Figure 2 have also been plotted and indicate a range in D between 1.0×10^{-12} and 5.0×10^{-10} mm^2/s. The error bars on plotted points represent the 10 µm diameter of the ion analysis spot.

Figure 5. Compositional profile for the replacement and host dolomite shown in Figure 3. (A) Back-scattered electron image of the replacement dolomite with the location of the section A–A′. The BSE image shows a sharp boundary between the host dolomite (dark) and Fe-bearing replacement dolomite (medium gray). Both the host and the replacement dolomite have numerous pores, $\sim$ 1 µm in diameter, and some Fe replacement can be seen around pores in the host dolomite. The locations of the SIMS analyses are also shown. (B) Concentration of FeO along the A–A′ section, showing a decreases from about 1.2 wt% at the right edge of the crystal, A′, to about 0.9% at the boundary between the replacement and host dolomite, to about 0.1 wt% in the host dolomite. The O-isotope values are also plotted, as projected along the section. F is elevated within the replacement, although the data are scattered, and near the grain boundary at its left edge.

This is a preprint, the final version is subject to change, of the American Mineralogist (MSA)
Cite as Authors (Year) Title. American Mineralogist, in press.
(DOI will not work until issue is live.) DOI: http://dx.doi.org/10.2138/am-2016-5635

Table 1. Sample MR6 Oxygen-Isotope SIMS Analyses

Spot Name	Mineral Type	Location	Average ^{16}O counts	Average ^{18}O counts	*F*
cc1	reaction-produced calcite	Figure 2 - Reaction zone	27372	5048	0.156
cc2	reaction-produced calcite	Figure 2 - Reaction zone	34736	5061	0.127
cc3	reaction-produced calcite	Figure 3 - Reaction zone	31536	5779	0.155
cc4	reaction-produced calcite	Figure 3 - Reaction zone	36372	6623	0.154
cc5	reaction-produced calcite	Figure 3 - Reaction zone	35094	5258	0.130
A1	unreacted dolomite	Figure 2 - Traverse A - grain rim	221477	917	0.004
A2	unreacted dolomite	Figure 2 - Traverse A	227659	546	0.002
A3	unreacted dolomite	Figure 2 - Traverse A	229025	453	0.002
A4	unreacted dolomite	Figure 2 - Traverse A	53180	103	0.002
A5	unreacted dolomite	Figure 2 - Traverse A	50775	99	0.002
B1	unreacted dolomite + reaction products	Figure 2 - Traverse B - grain rim	47335	7733	0.140
B2	unreacted dolomite	Figure 2 - Traverse B	49181	398	0.008
B3	unreacted dolomite	Figure 2 - Traverse B	49581	97	0.002
B4	unreacted dolomite	Figure 2 - Traverse B	49224	92	0.002
C1	unreacted dolomite	Figure 2 - Traverse C - grain rim	86361	1361	0.016
C2	unreacted dolomite	Figure 2 - Traverse C	70818	317	0.004
C3	unreacted dolomite	Figure 2 - Traverse C	61600	151	0.002
C4	unreacted dolomite	Figure 2 - Traverse C	58521	115	0.002

This is a preprint, the final version is subject to change, of the American Mineralogist (MSA)
Cite as Authors (Year) Title. American Mineralogist, in press.
(DOI will not work until issue is live.) DOI: http://dx.doi.org/10.2138/am-2016-5635

Spot Name	Mineral Type	Location	Average ^{16}O counts	Average ^{18}O counts	*F*
D1	unreacted dolomite	Figure 3 - Traverse D - grain rim	205401	10540	0.049
D2	unreacted dolomite	Figure 3 - Traverse D	224180	462	0.002
D3	unreacted dolomite	Figure 3 - Traverse D	224670	441	0.002
E1	Fe dolomite	Figure 3 - Traverse E - grain rim	177845	4360	0.024
E2	Fe dolomite	Figure 3 - Traverse E	218095	5033	0.023
E3	Fe dolomite	Figure 3 - Traverse E	222613	4659	0.020
F1	Fe dolomite + reaction products	Figure 3 - Traverse F - grain rim	23550	1680	0.067
F2	Fe dolomite	Figure 3 - Traverse F	44868	150	0.003
F3	Fe dolomite + reaction products	Figure 3 - Traverse F	42925	1669	0.037
F4	unreacted dolomite	Figure 3 - Traverse F	49407	99	0.002
F5	unreacted dolomite	Figure 3 - Traverse F	44099	104	0.002
F6	unreacted dolomite	Figure 3 - Traverse F	39495	2325	0.056
G1	reaction products	Figure 3 - Traverse G - grain rim	37906	5818	0.133
G2	Fe dolomite	Figure 3 - Traverse G	39580	978	0.024
G3	Fe dolomite	Figure 3 - Traverse G	43578	600	0.014
G4	unreacted dolomite	Figure 3 - Traverse G	45146	114	0.003
G5	unreacted dolomite	Figure 3 - Traverse G	41896	358	0.008
G6	unreacted dolomite + reaction products	Figure 3 - Traverse G	42298	662	0.015

This is a preprint, the final version is subject to change, of the American Mineralogist (MSA)
Cite as Authors (Year) Title. American Mineralogist, in press.
(DOI will not work until issue is live.) DOI: http://dx.doi.org/10.2138/am-2016-5635

Table 2. O mass balance for experiment MR 6

		Mass (mg)	^{18}O (mg)	^{16}O (mg)	Notes
Start					
	HDO[1]	38.05	17.12	15.22	
	Dolomite	237.75	0	123.77	Assumed to be all ^{16}O
	Total	275.80	17.12	138.99	
Finish					
	HDO[1]	38.05	13.40	17.41	Calculated by difference
	CO_2	10.78		7.84	Assumed to be all ^{16}O from dolomite
	Dolomite	192.58	1.25	99.00	Calculated from diffusion solution
	Loss to fluid			1.25	Calculated from diffusion solution
	Periclase	9.87	0.62	3.37	Atom fraction assumed to be the same as in calcite
	Calcite	24.52	1.85	10.11	From measured atom fraction of 0.14
	Total	275.80	17.12	138.99	
	Fluid $^{18}O/(^{18}O + ^{16}O)$ by weight			0.34	
	Fluid $^{18}O/(^{18}O + ^{16}O)$ by atom			0.31	

Note: [1]Fluid composition is $HD^{18}O_{0.5}{}^{16}O_{0.5}$

This is a preprint, the final version is subject to change, of the American Mineralogist (MSA)
Cite as Authors (Year) Title. American Mineralogist, in press.
(DOI will not work until issue is live.) DOI: http://dx.doi.org/10.2138/am-2016-5635

DeAngelis et al. Figure 1

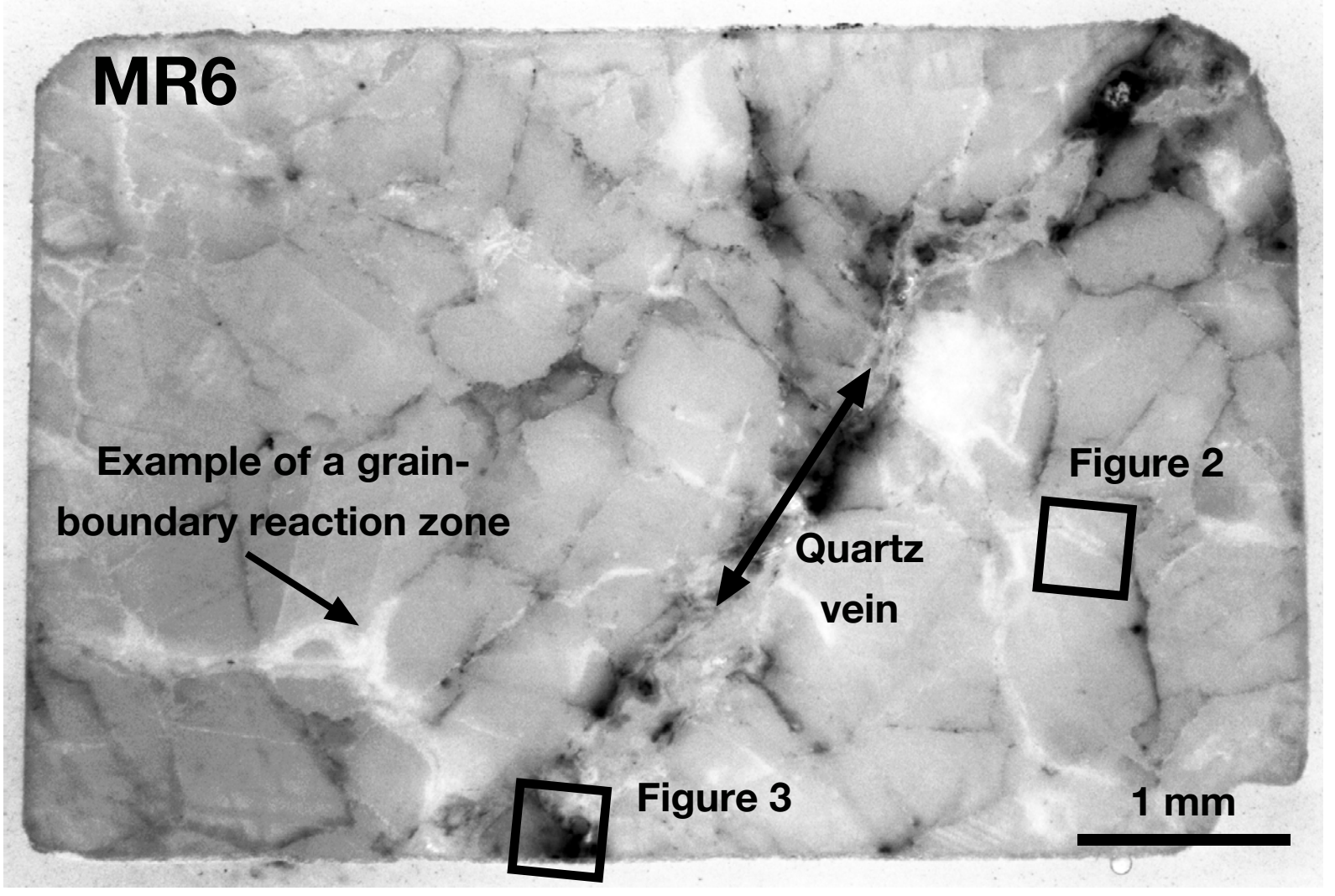

This is a preprint, the final version is subject to change, of the American Mineralogist (MSA)
Cite as Authors (Year) Title. American Mineralogist, in press.
(DOI will not work until issue is live.) DOI: http://dx.doi.org/10.2138/am-2016-5635

DeAngelis et al. Figure 2

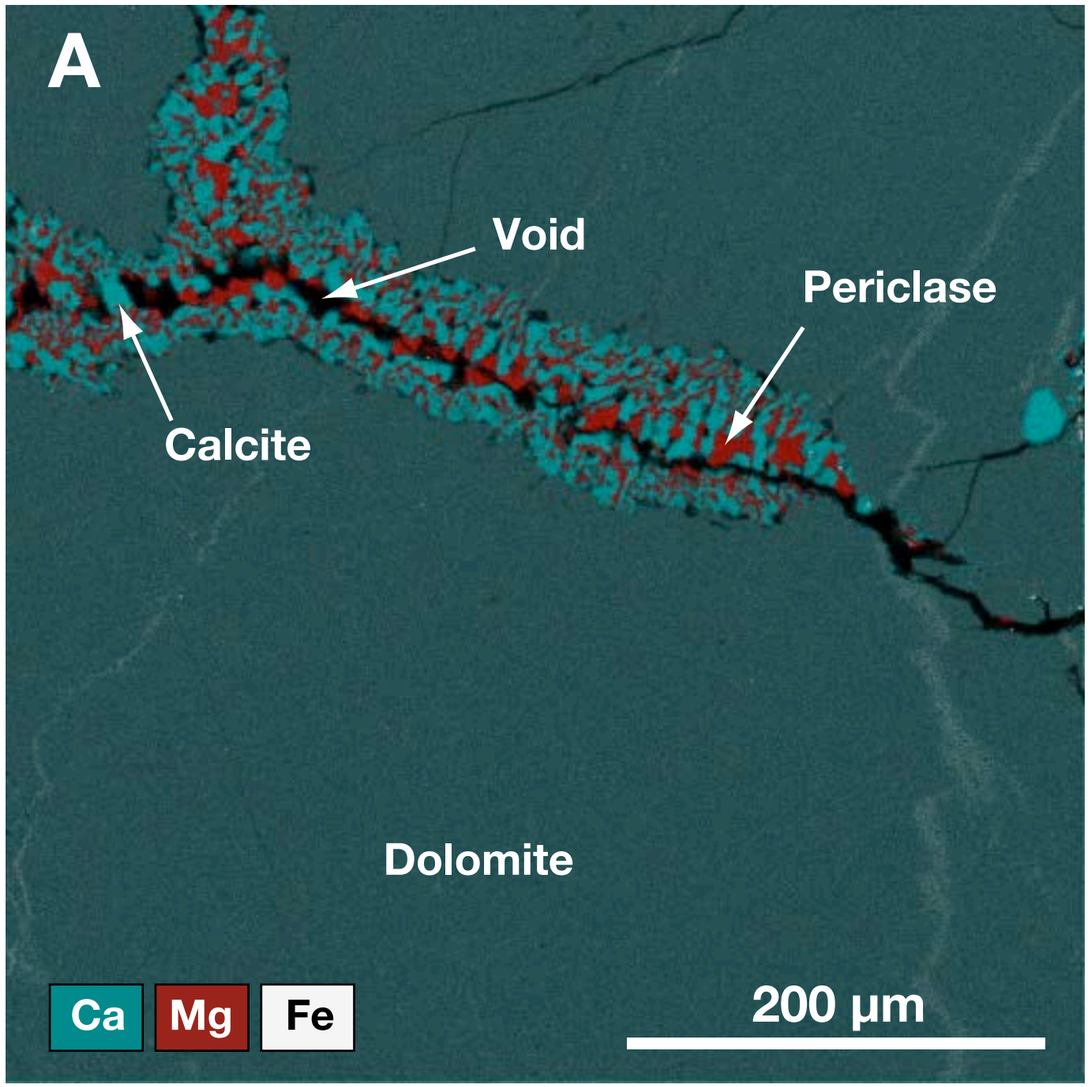

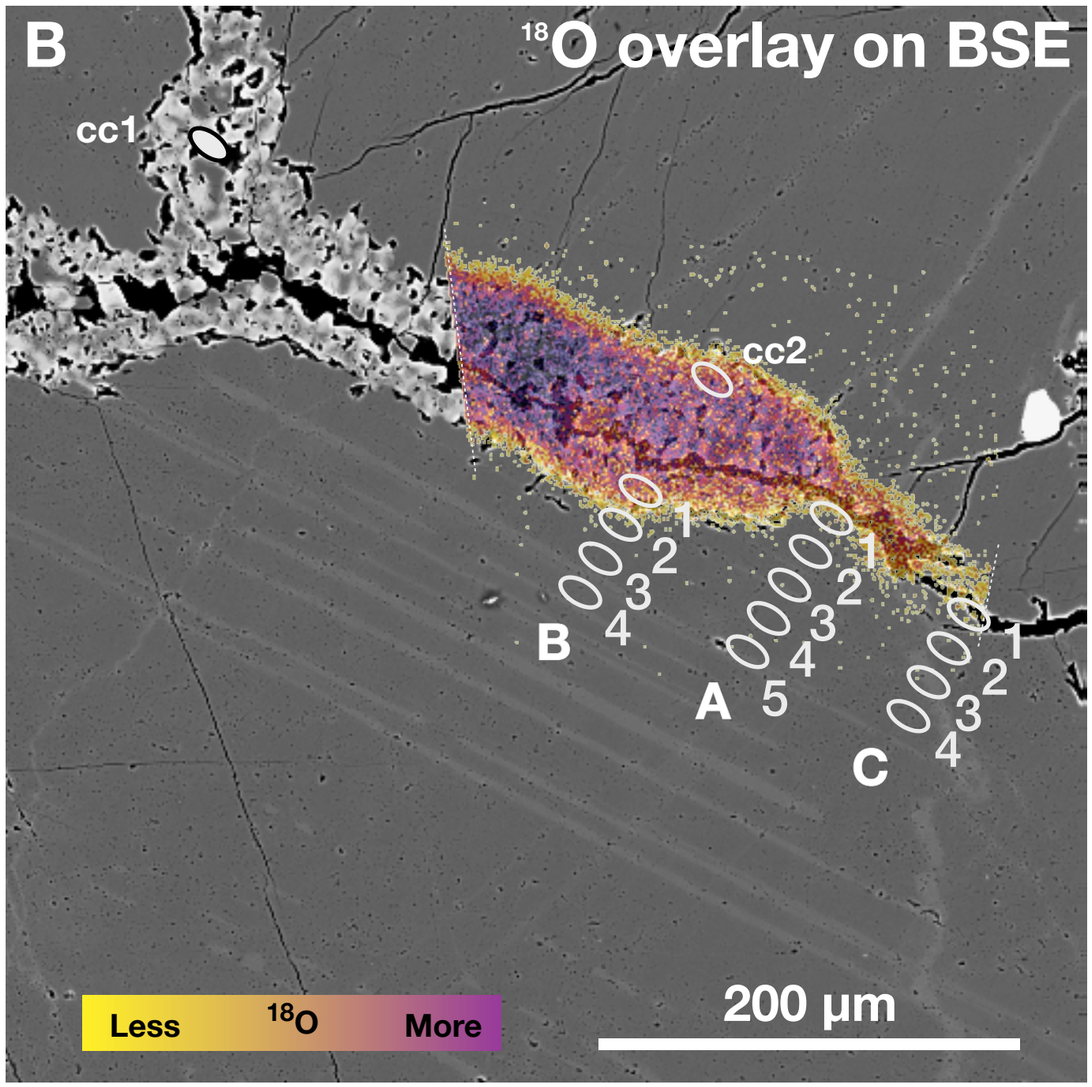

This is a preprint, the final version is subject to change, of the American Mineralogist (MSA)
Cite as Authors (Year) Title. American Mineralogist, in press.
(DOI will not work until issue is live.) DOI: http://dx.doi.org/10.2138/am-2016-5635

DeAngelis et al. Figure 3

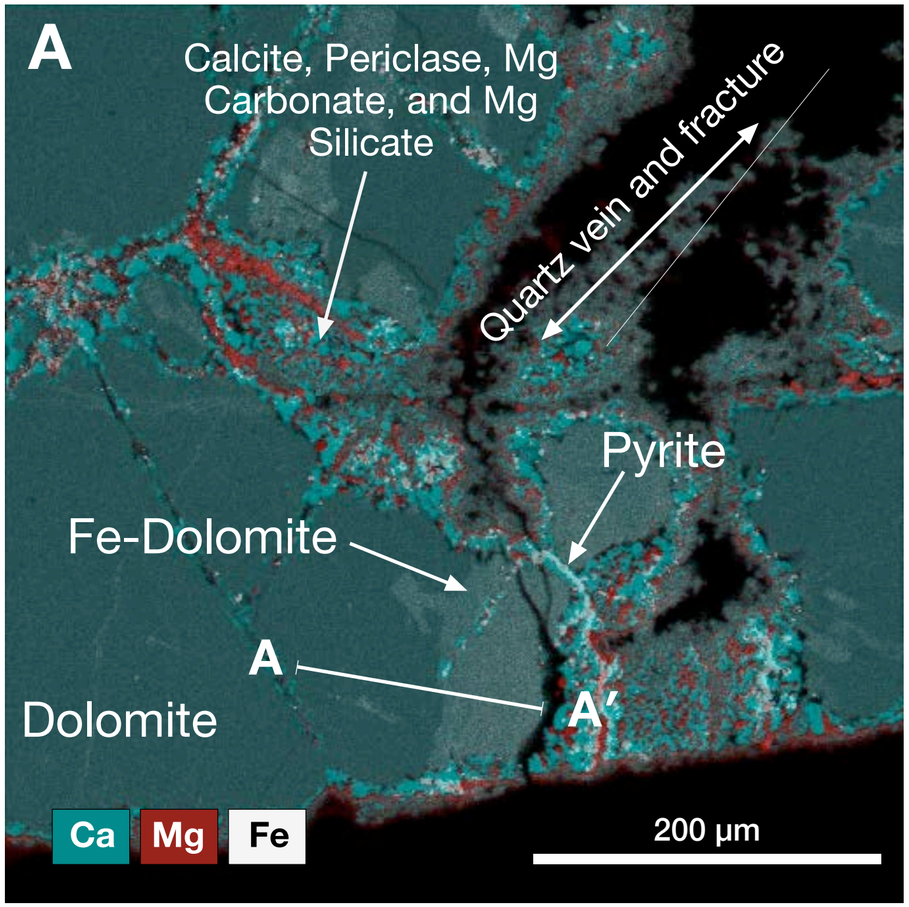

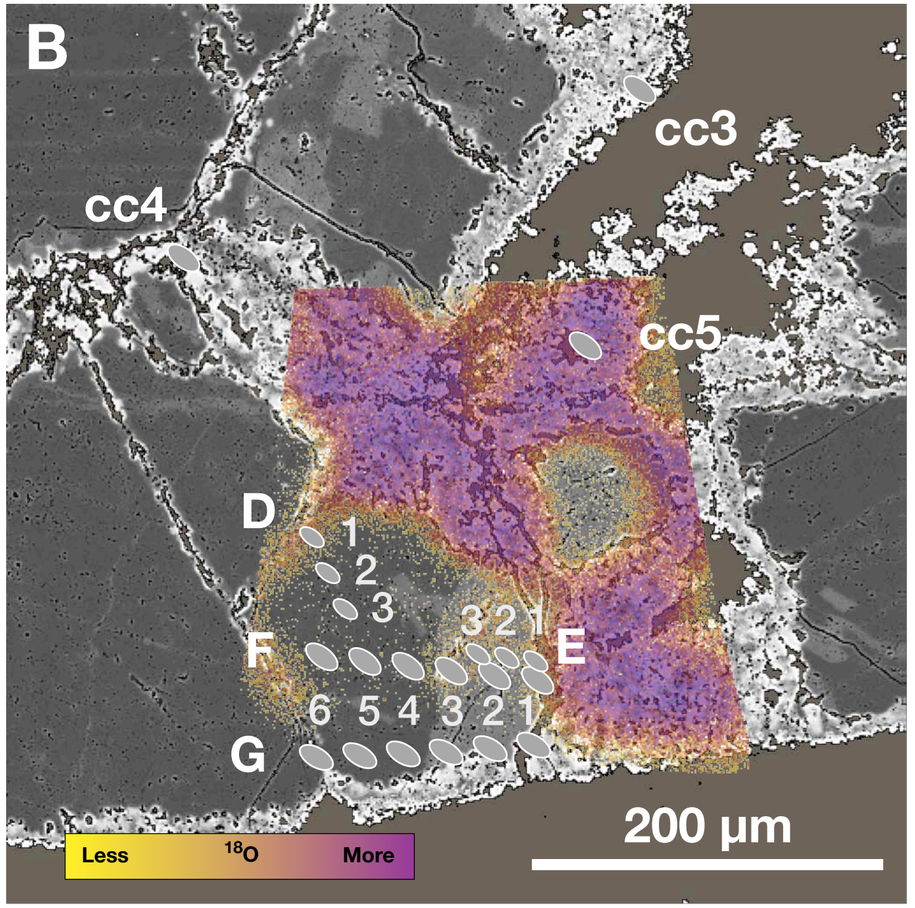

This is a preprint, the final version is subject to change, of the American Mineralogist (MSA)
Cite as Authors (Year) Title. American Mineralogist, in press.
(DOI will not work until issue is live.) DOI: http://dx.doi.org/10.2138/am-2016-5635

DeAngelis et al. Figure 4

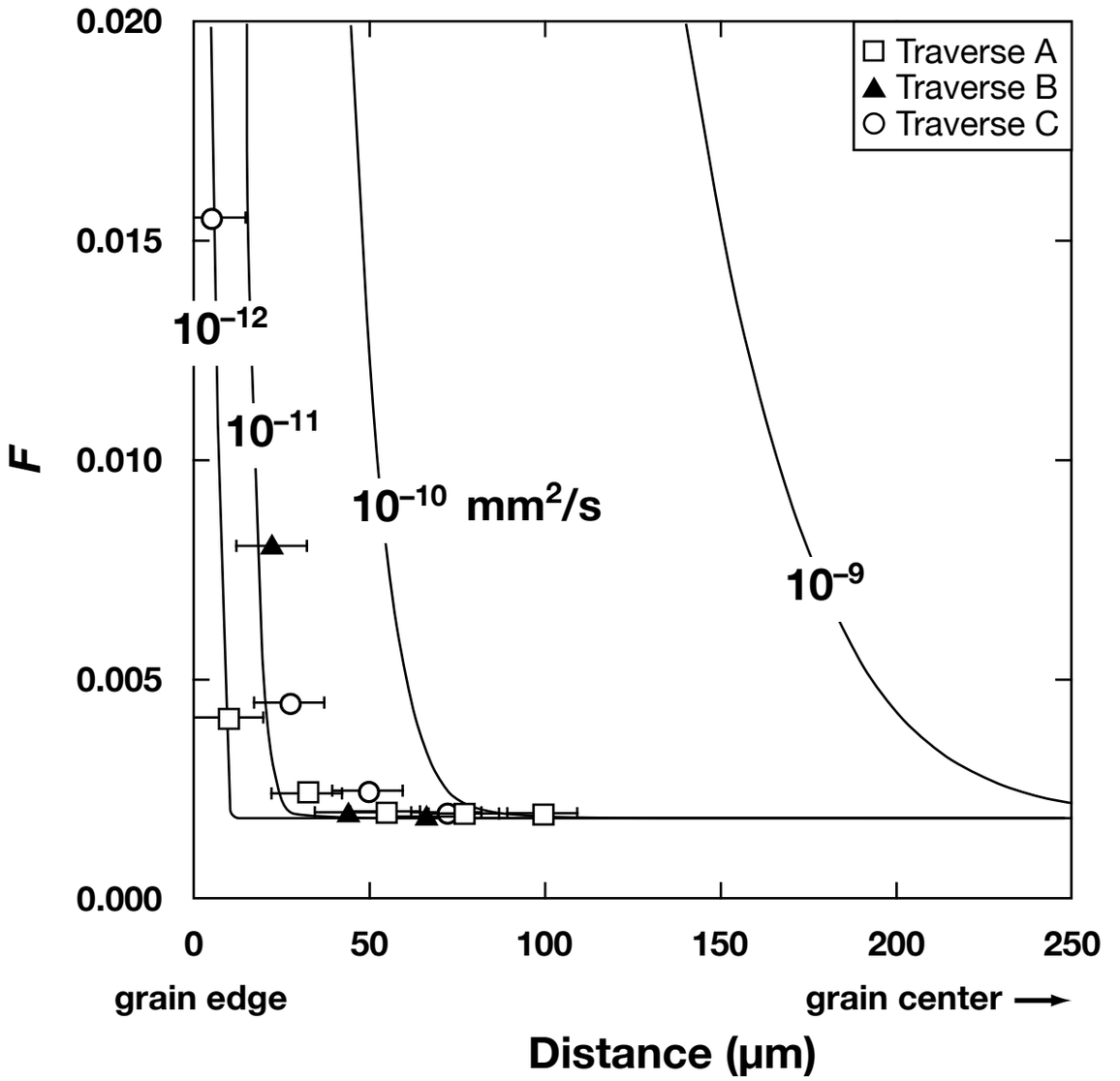

This is a preprint, the final version is subject to change, of the American Mineralogist (MSA)
Cite as Authors (Year) Title. American Mineralogist, in press.
(DOI will not work until issue is live.) DOI: http://dx.doi.org/10.2138/am-2016-5635

DeAngelis et al. Figure 5